

**The ability of the ground penetrating radar in subsurface pipes situation  
identification: computer simulations**

<https://doi.org/10.32792/utq/utj/vol10/3/4>

Hussein K. Chlaib<sup>1</sup>, Najah Abd<sup>2</sup>, Ali Ramthan Hussein<sup>3</sup>

<sup>1</sup> Thi-Qar university, College of Science, Department of Physics, Thi-Qar, Iraq,  
[hkaldobayany@yahoo.com](mailto:hkaldobayany@yahoo.com), [hkchlaib@ualr.edu](mailto:hkchlaib@ualr.edu).

<sup>2</sup> University of Baghdad, College of Science, Department of geology, Baghdad,  
Iraq, [naabd@ualr.edu](mailto:naabd@ualr.edu).

<sup>3</sup> Ministry of education, [aliramthan@yahoo.com](mailto:aliramthan@yahoo.com).

**Abstract**

Nowadays, the subsurface pipe leaks are one of the important and common pipe problems in Iraq; these pipes are difficult to detect and locate for fixing or replacing. As it is known, the geophysical methods play a major role to detect subsurface targets. Ground penetrating radar (GPR) is one of the geophysical tools that detect the subsurface targets.

Before applying this technique in the field, the computer simulations will take place. Several synthetic models have been simulated to study the GPR effectiveness and its ability to detect and identify the subsurface pipes situation and parameters (depth, size, filled materials). GPRMax2D V2.0 software was used in these simulations. These models consist of many synthetic pipes with various sizes, depths and filled materials, which were air, clay and water.

The simulations showed that GPR was able to detect the subsurface pipes and identify their parameters (size/shape/depth and filled materials).

Key words: Dielectric constant, Filled materials, GPRMax2D, pipes Simulations.

## **Introduction**

Due to the infrastructure destruction in Iraq after all the wars that happened in the past and present times, Iraq starts reconstruction. One of the important infrastructure, the subsurface water pipes. This specific infrastructure always faces the leak problem. The common present way to locate these subsurface pipe leaks is digging the surface randomly and destroys the pavements and walkways. Here, the geophysical investigation methods will play the effective role to fix these problems. These methods are noninvasive, as well as they prevent the time and cost consuming. One of these methods is the GPR, which is one of the electromagnetic geophysical methods. The computer simulation software is easy tools to understand any situation before dealing with the real field. GPRMax is a set of electromagnetic wave simulation tools based on the Finite-Difference Time-Domain (FDTD) numerical method (Yee, 1966). GPRMax was originally developed in 1996 when numerical modeling using the FDTD method and, in general, the numerical modeling of GPR were in their infancy.

The FDTD modeling technique has the advantages of being relatively simple to implement and allows a better interpretation of the physical phenomena. During the last twenty five years, many papers on GPR data modeling have been published (e.g., Roberts & Daniels, 1996; Xu & McMechan, 1997; and Teixeira et al, 1998). Luebbbers & Hunsberger (1992)

presented a FDTD technique for EM waves modeling of Nth-order dispersive media; Carcione(1996) and Carcione& Schoenberg(2000) applied a similar formalism for GPR data modeling in dispersive and anisotropic media. The radiation pattern of antennas has been modeled by using the FDTD technique with different geometries including the air-soil interface effect (e.g.,Carcione 1998, Lampe et al., 2003).

GPRMax consists of two simulators, GPRMax2D and GPRMax3D, the first one solves the transverse-magnetic mode with respect to  $z$  (TM  $z$ ) in 2D, while the second one solves the full FDTD algorithm in 3D. Due to that both simulators are command-line-driven programs that do not feature a graphical user interface (GUI), GPRMax will be very flexible and scriptable software that can be easily used in many different applications. It specifically allows GPRMax to be run in high-performance computing (HPC) environments, i.e. on supercomputers (Su, 2013). GPRMax contains many powerful and flexible features such as, Perfectly Matched Layer (PML) absorbing boundary conditions, user-definable materials, user-specifiable excitation functions, simulation of thin wires, as well as voltage sources and 1D transmission line models for feeding antennas.

After reviewing the previous works, especially in Iraq, and according to the authors' information, it is probable to say that no any researcher used the GPRMax modeling to identify the subsurface pipes situation which is very important subject in Iraq.

### **The GPR data modeling**

A two-dimension (2-D) FDTD procedure was adopted to simulate different subsurface pipe settings. Six synthetic models were designed to simulate various subsurface conditions that include subsurface pipes filled with various materials and within one host media. These models were simulated to see the electromagnetic wave reflection and behaviors when it interacts with. A rectangular block was used as the initial model for simulation with

dimensions of 2.50m along the x-axis and 1.75m along the y-axis. The incident pulse is Gaussian in the time domain with a bandwidth of 900 MHz. A probe was placed at the surface to monitor reflections produced by the object interfaces. For all of the models, the host medium was clayey sand with a dielectric constant of ( $\epsilon$ )= 6, Table 1 shows the dielectric constants for many common materials.

Table 1: The dielectric constants for common materials, modified after Reynolds, 1998.

<b>Material</b>	<b>Dielectric constant, <math>\epsilon</math></b>	<b>Material</b>	<b>Dielectric constant, <math>\epsilon</math></b>
<b>Air</b>	<b>1</b>	<b>Wet clay</b>	<b>8-15</b>
<b>Water</b>	<b>80</b>	<b>Dry clay soil</b>	<b>3</b>
<b>Polar snow</b>	<b>1.4-3</b>	<b>Agricultural land</b>	<b>15</b>
<b>Polar ice</b>	<b>3-3.15</b>	<b>Granite</b>	<b>5-8</b>
<b>Dry sand</b>	<b>3-6</b>	<b>Coal</b>	<b>4-5</b>
<b>Wet sand</b>	<b>25-30</b>	<b>Quartz</b>	<b>4.3</b>
<b>Wet silt</b>	<b>10</b>	<b>Concrete</b>	<b>3-5</b>
<b>Asphalt</b>	<b>3-5</b>	<b>PVC</b>	<b>3</b>

The six models had shown as below:

The first model:The simulated pipe in the first model was an air-filled pipe ( $\epsilon=1$ ) simulated within this medium with a center coordinates of (1.25 m 1.05 m) and a diameter of 0.05m. Figure (1) represents the geometry of this model while Figure (2) shows the synthetic results (row data) of the same model the air-filled pipe

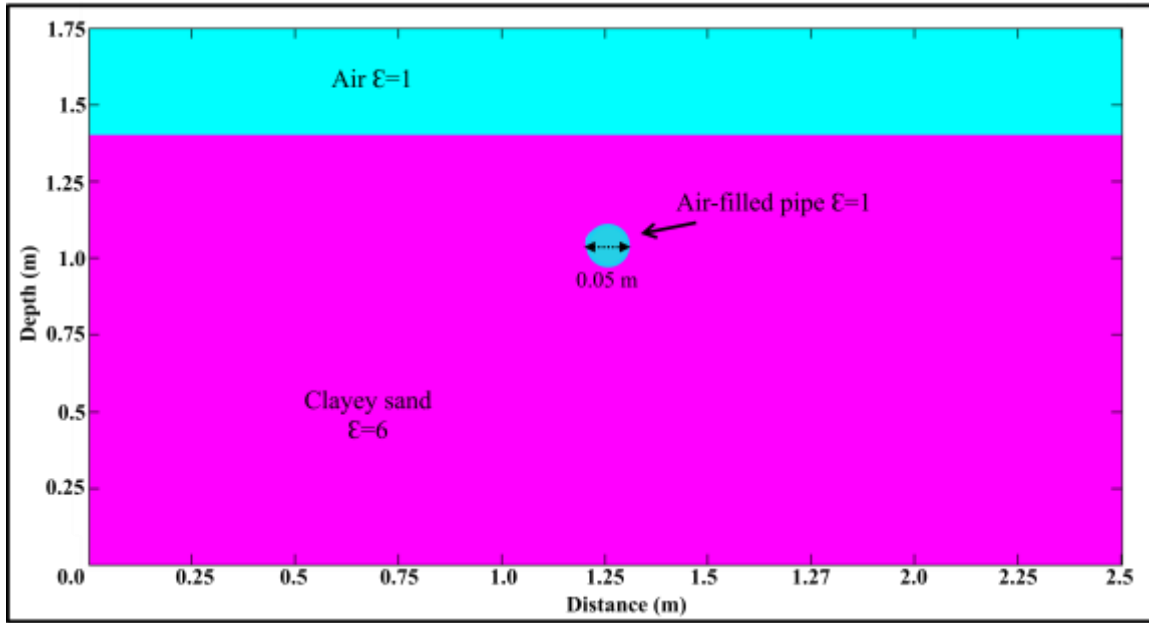


Figure (1):The geometry of the first model

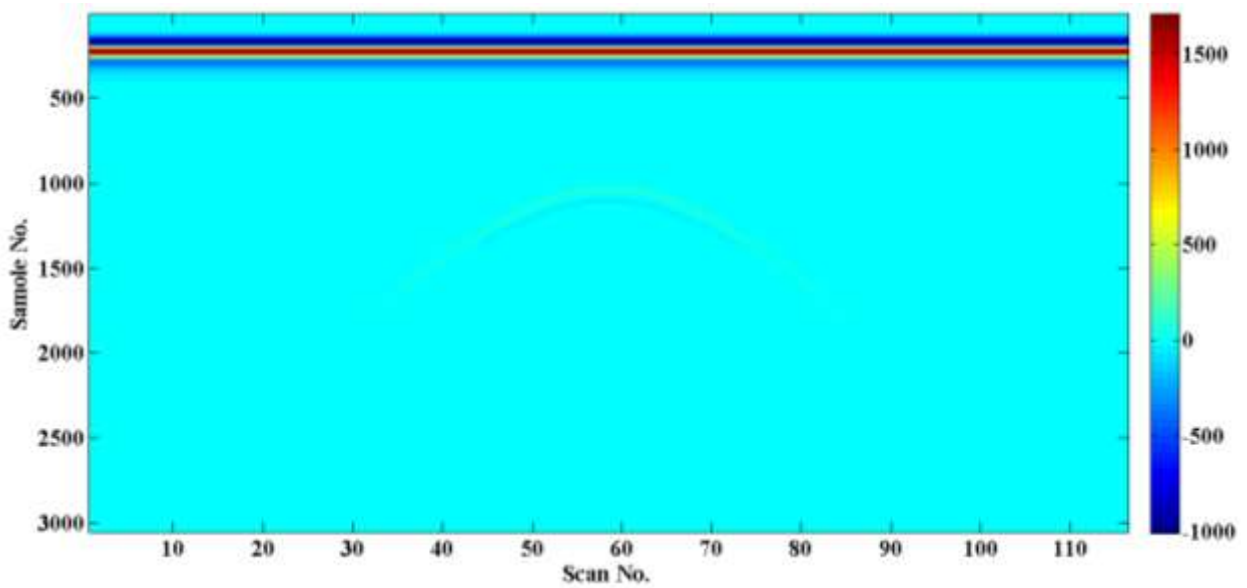


Figure (2):The synthetic results (row data) of the same model which is shown in Figure 1(the air-filled pipe)

The second model:In this model, water-filled pipe ( $\epsilon=80$ ) was simulated within the clayey sand medium with a center coordinates of (1.25m, 1.05 m) and a diameter of 0.05m as showed in figure (3) which represents the geometry of this model while figure (4) shows the synthetic results the water-filled pipemodel.

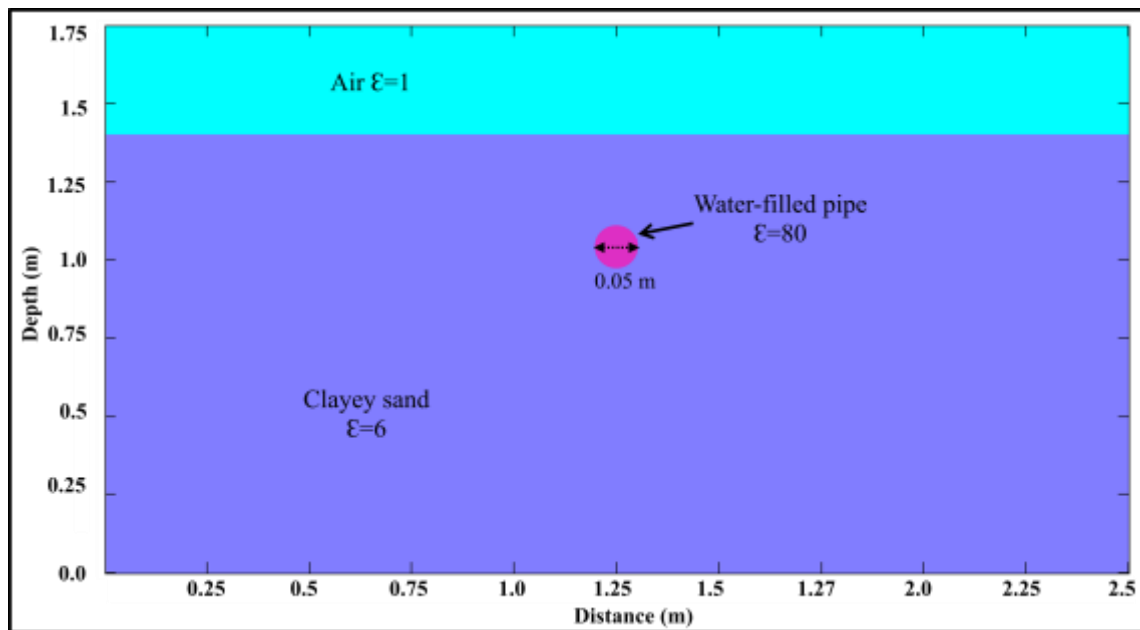


Figure (3):The geometry of the second model (Water-filled pipe)

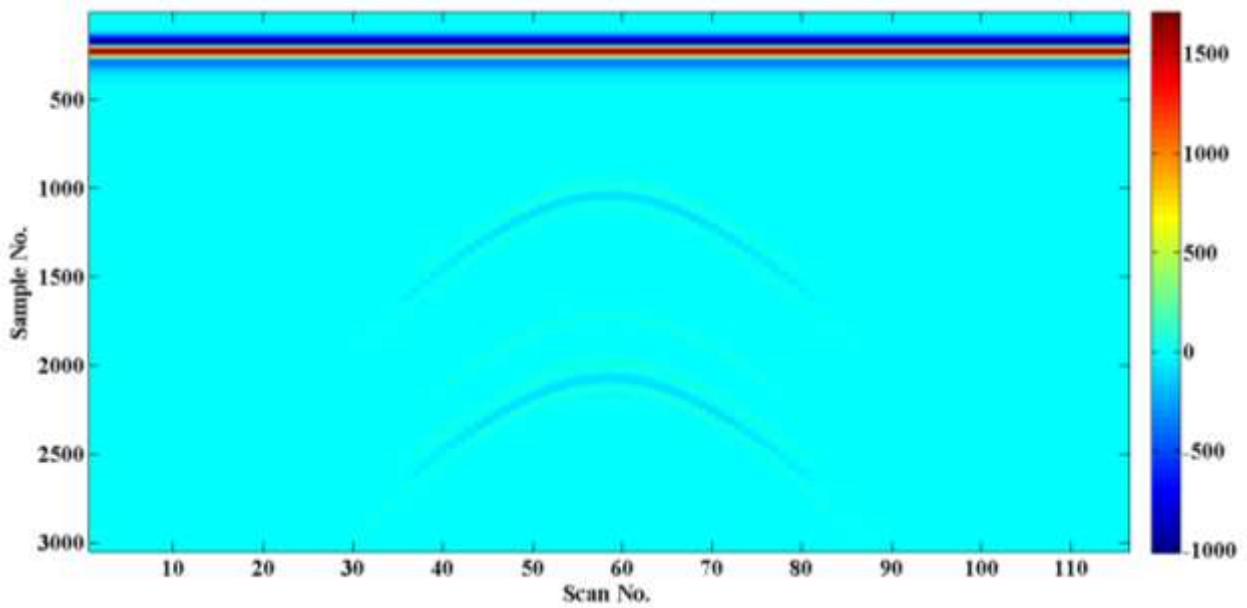


Figure (4):The synthetic results (row data) of the water-filled pipemodel

The third model:In this model, common problem in the subsurface pipes was represented. A clay-filled pipe ( $\epsilon=10$ ) was simulated within this medium with a center coordinates of (1.25 m, 1.05m). Its diameter is 0.05m. Figure (5) represents the geometry of this model showed in figure 5, while the synthetic results of it showed in figure 6.

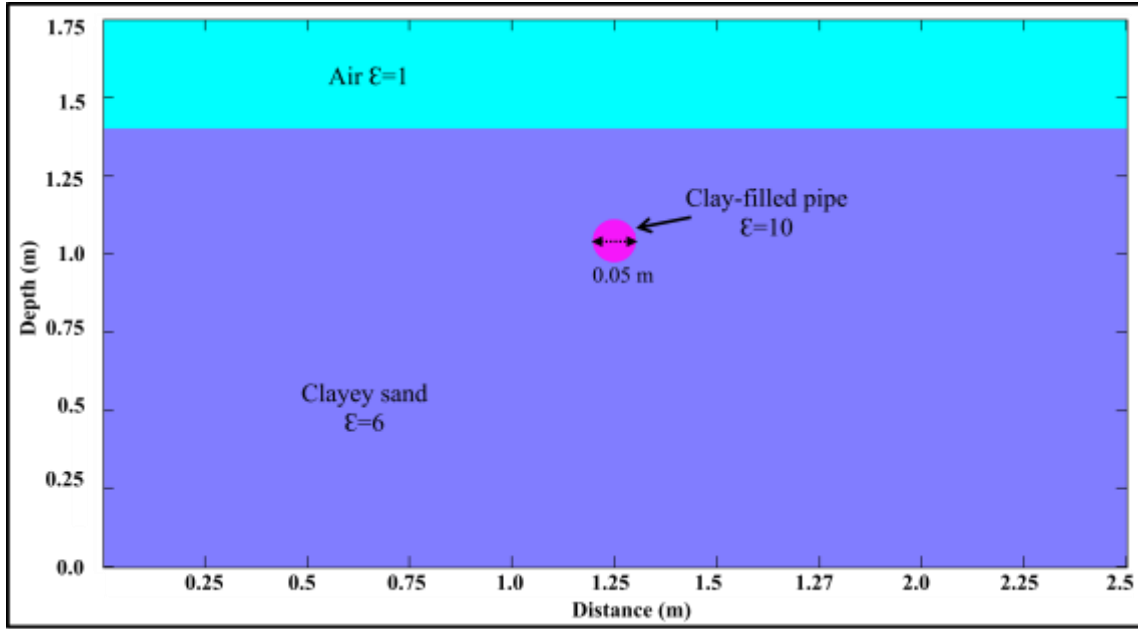


Figure (5):The geometry of third model (Clay-filled pipe)

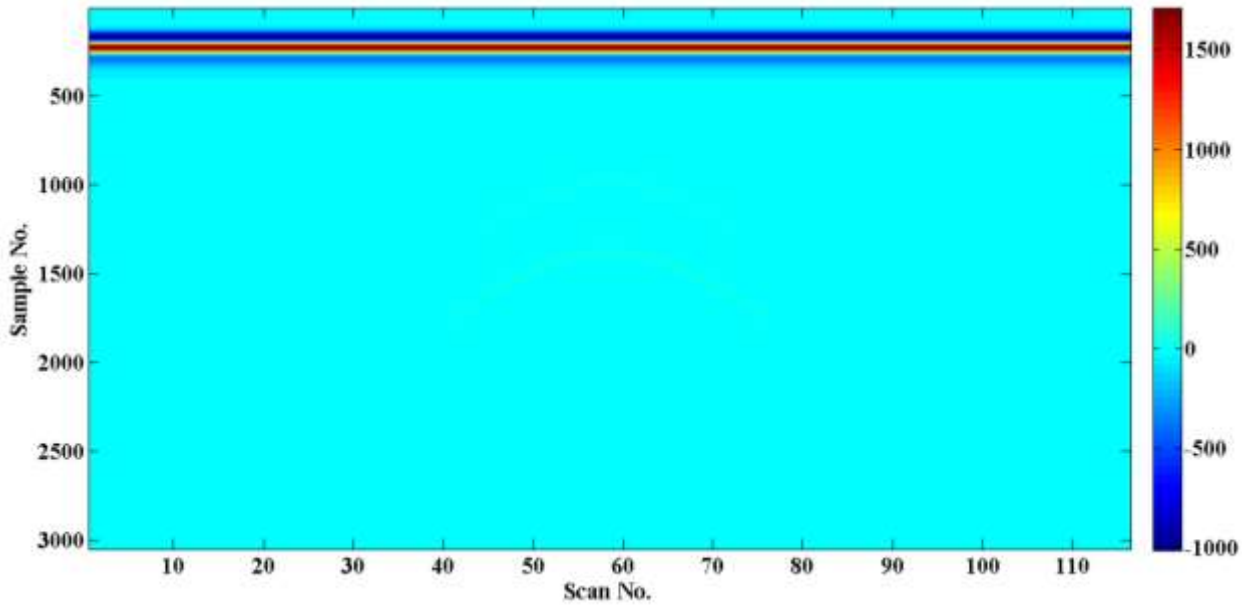


Figure (6):The synthetic results of the clay-filled pipemodel.

The fourth model:This model consists of three simulated subsurface pipes have different sizes and located under varies depths. A clay-filled pipe, water-filled pipe, and an air-filled pipe



with dielectric constants of ( $\epsilon=10, 80, \text{ and } 1$ ), depth of the center coordinates on the X and Y axes are ((0.5m, 0.35m), (1.3m, 0.70m), and (2.1m, 1.05m)), and they have diameters of (0.15m, 0.10m, and 0.5m) respectively. The horizontal distance between the clay-filled and water-filled pipes was 0.675 m and between the water-filled and air-filled pipes was 0.725 m (between the pipe outer sides), while the horizontal distance between the pipes centers was 0.80 m. The vertical distance between the pipe centers was 0.35 m. Figure (7) represents the geometry of this model and figure (8) shows the synthetic results of it.

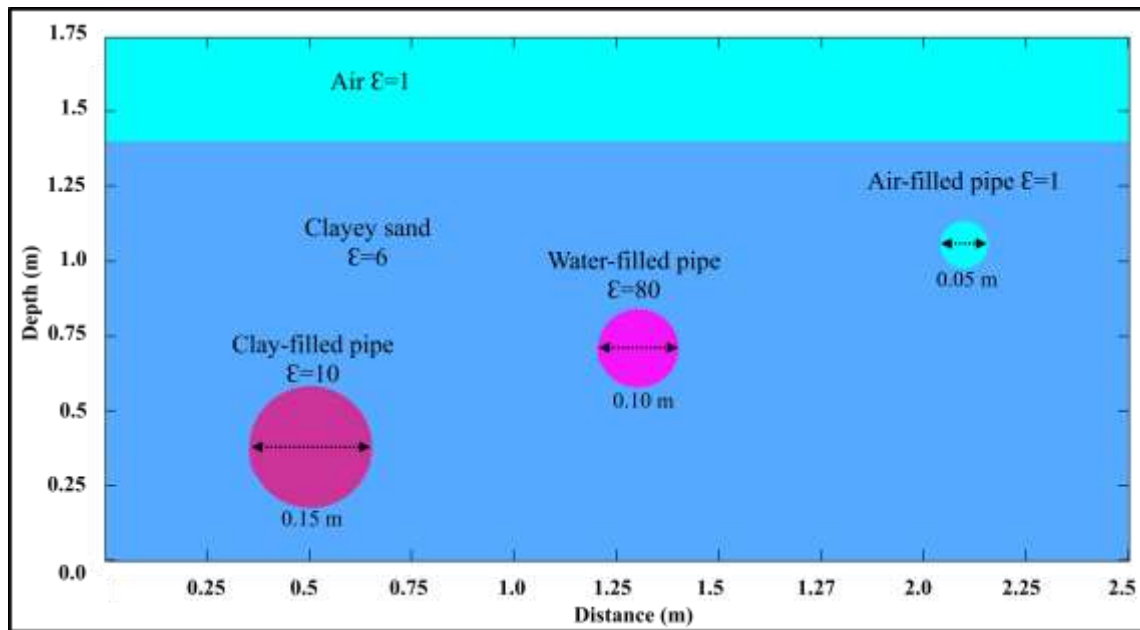


Figure (7):The geometry of forth model.

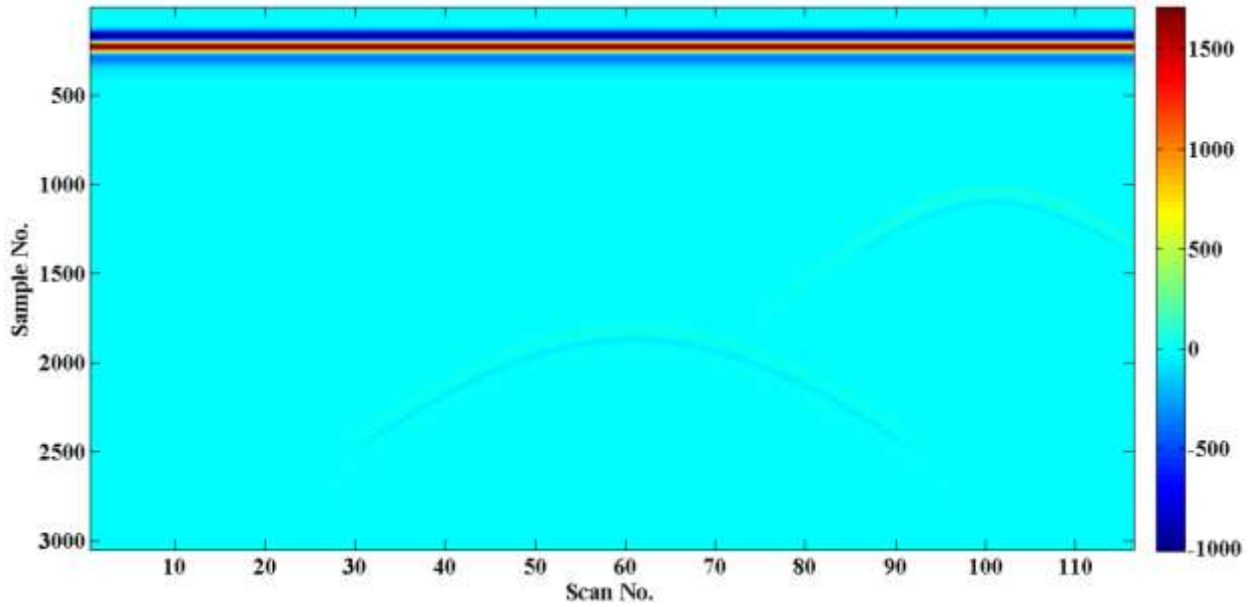


Figure (8):The synthetic results of the same model, clay-filled pipe, water-filled pipe, and air-filled pipe have different diameters and placed at different depths

The fifth model: This model is as same as the forth one except all the pipes have same diameters which is 0.05 m which showed in figure (9) that represents the geometry of this model and figure (10) shows the synthetic results.

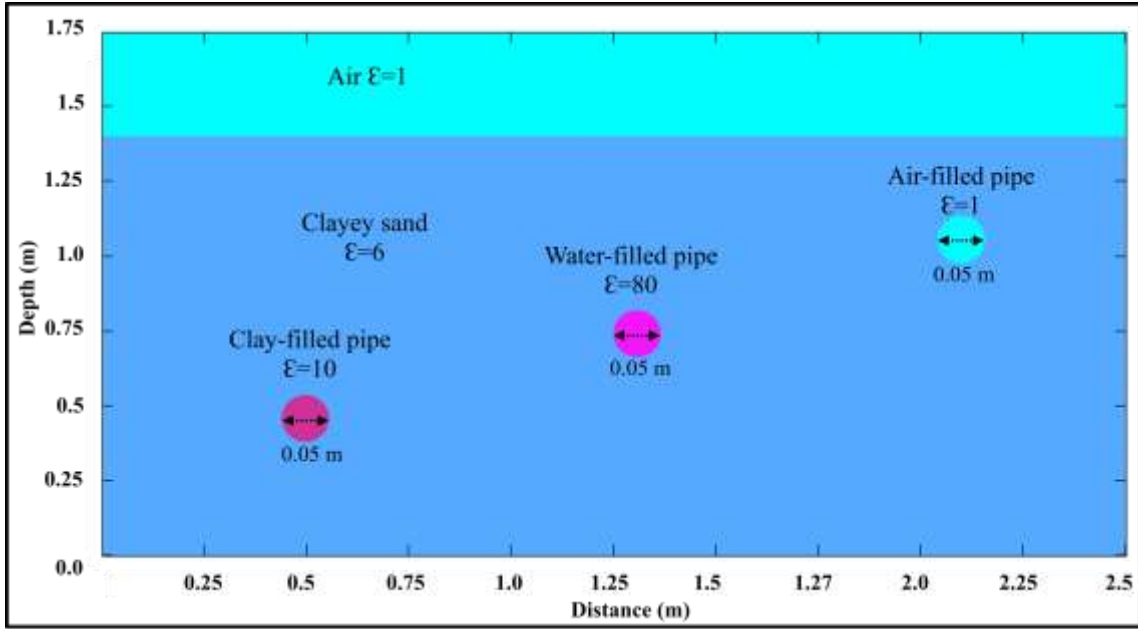


Figure (9):The geometry of the fifth model

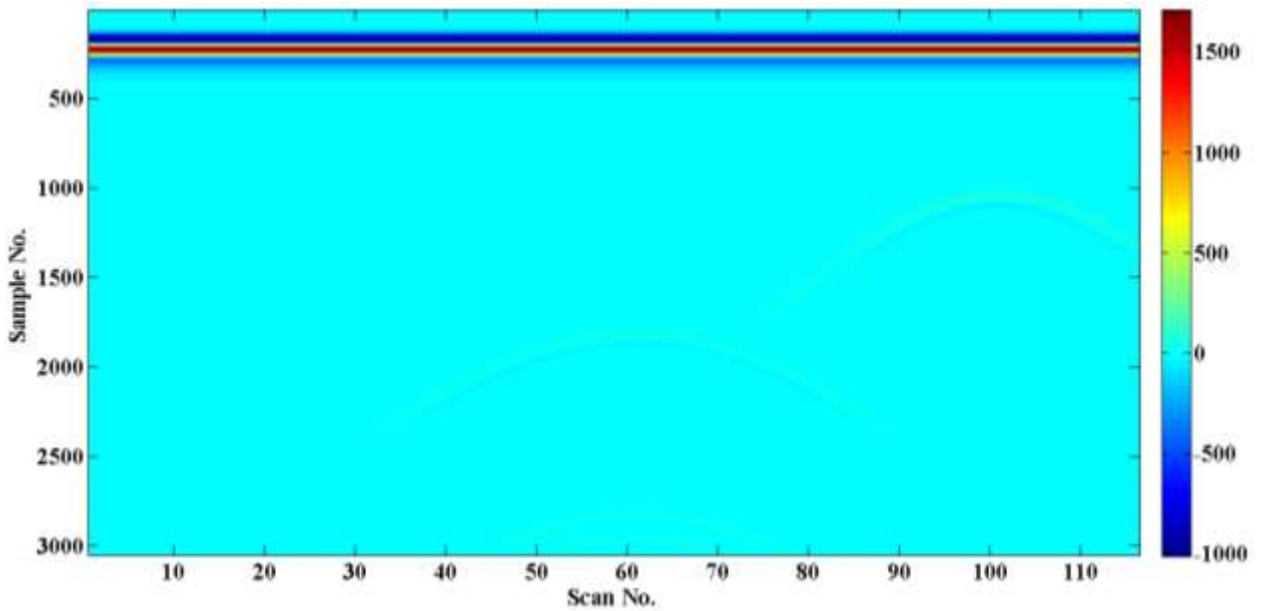


Figure (10):The synthetic results of the fifth model, clay-filled pipe, water-filled pipe, and air-filled pipe have same diameters and placed in different depths.

The sixth model: This model consists of three simulated subsurface pipes. Clay-filled, water-filled, and an air-filled pipe with dielectric constants of ( $\epsilon=10, 80, \text{ and } 1$ ), the depth of the center coordinates of  $((0.5, 0.95), (1.3, 1.00), \text{ and } (2.1, 1.05))$  respectively, the pipe diameters were 0.15, 0.10, and 0.05 respectively. The upper sides of these pipes are located at the same depth. Figure (11) represents the geometry of this model while figure (12) shows the synthetic results of the sixth model.

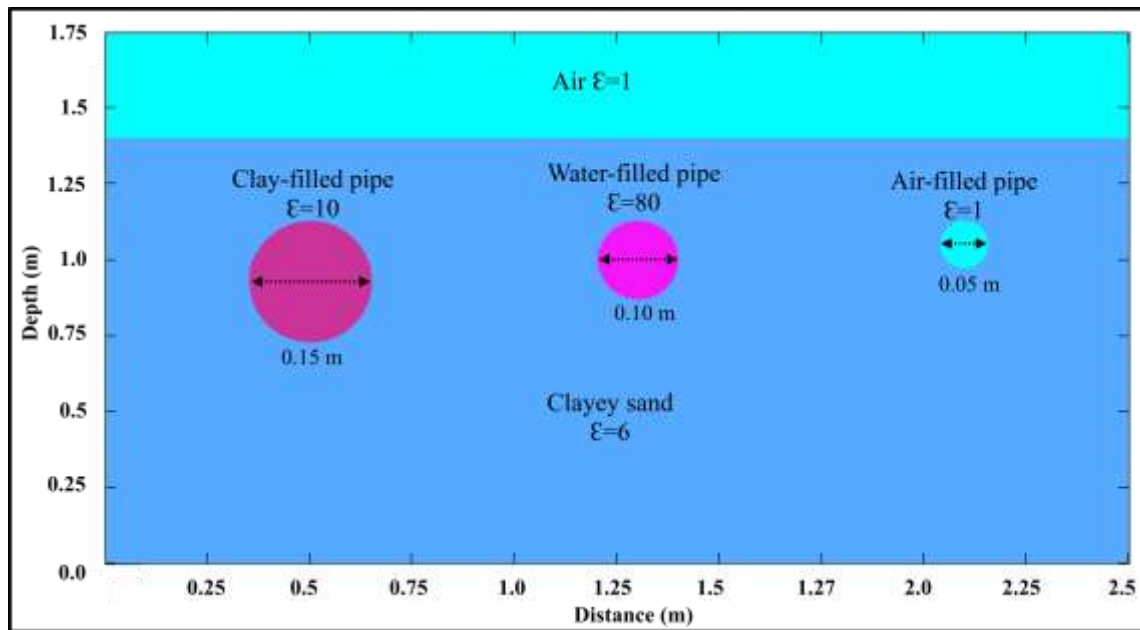


Figure (11):The geometry of the sixth model.

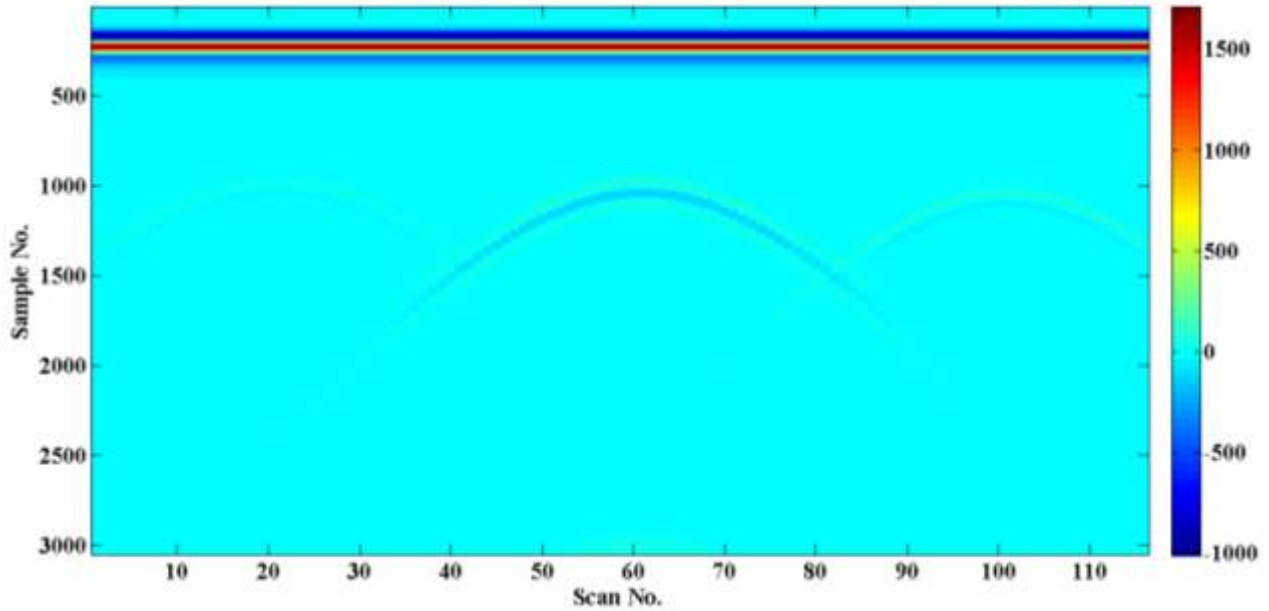


Figure (12): The synthetic results of the sixth model, clay-filled, water-filled, and air-filled pipes have different diameters and placed in same depths

## Results and discussion

In general, all the simulated subsurface pipes were located by the simulated GPR electromagnetic waves and the reflected waves from them are so clear. The 900MHz antenna was chosen due to its high resolution and the relative shallow penetration depth (reference). The synthetic data of first model (air-filled pipe) which represent an empty pipe shows a clear reflection at a depth corresponding to the samples of approximately 1000. The electromagnetic wave behavior when it reflected from a target with low dielectric constant shows a large peak (amplitude  $\approx 50$ ) in the positive side, which is clear by comparing the color in the figure (2). Also, the lower boundary of the pipe was hard to locate. Figure 13 (a) shows one scan across the air-filled pipe, note the highest peak located in the positive side.

The synthetic data of the second model which represent water-filled pipe shows the reflection from the pipe. Due to the high reflection coefficient between the clayey sand and the water, the reflection is very clear and there is a large negative apex (amplitude  $\approx -70$ ). Also, there is another very high reflection at a sample number of 2350, the color sequence is as same as the first reflection, and this is a phenomenon called the reverberation because of the high value of the reflection coefficient between the two mediums; big amount of the electromagnetic wave will reflect to the surface and redirected to the subsurface and so on (Olhoeft, 2003). Figure 13(b) shows a scan across a subsurface water-filled pipe.

The synthetic data of the third model, which represent a common pipe problem which is clay-filled pipe, shows the reflection from the pipe. Due to the reflection coefficient value between the clayey sand and the clay (which is less than the previous state), the reflection is clear and there is a large negative apex (amplitude  $\approx -15$ ). Also, there is another high reflection at a sample number of 1760. Figure 13 (c) shows a scan across a subsurface water-filled pipe.

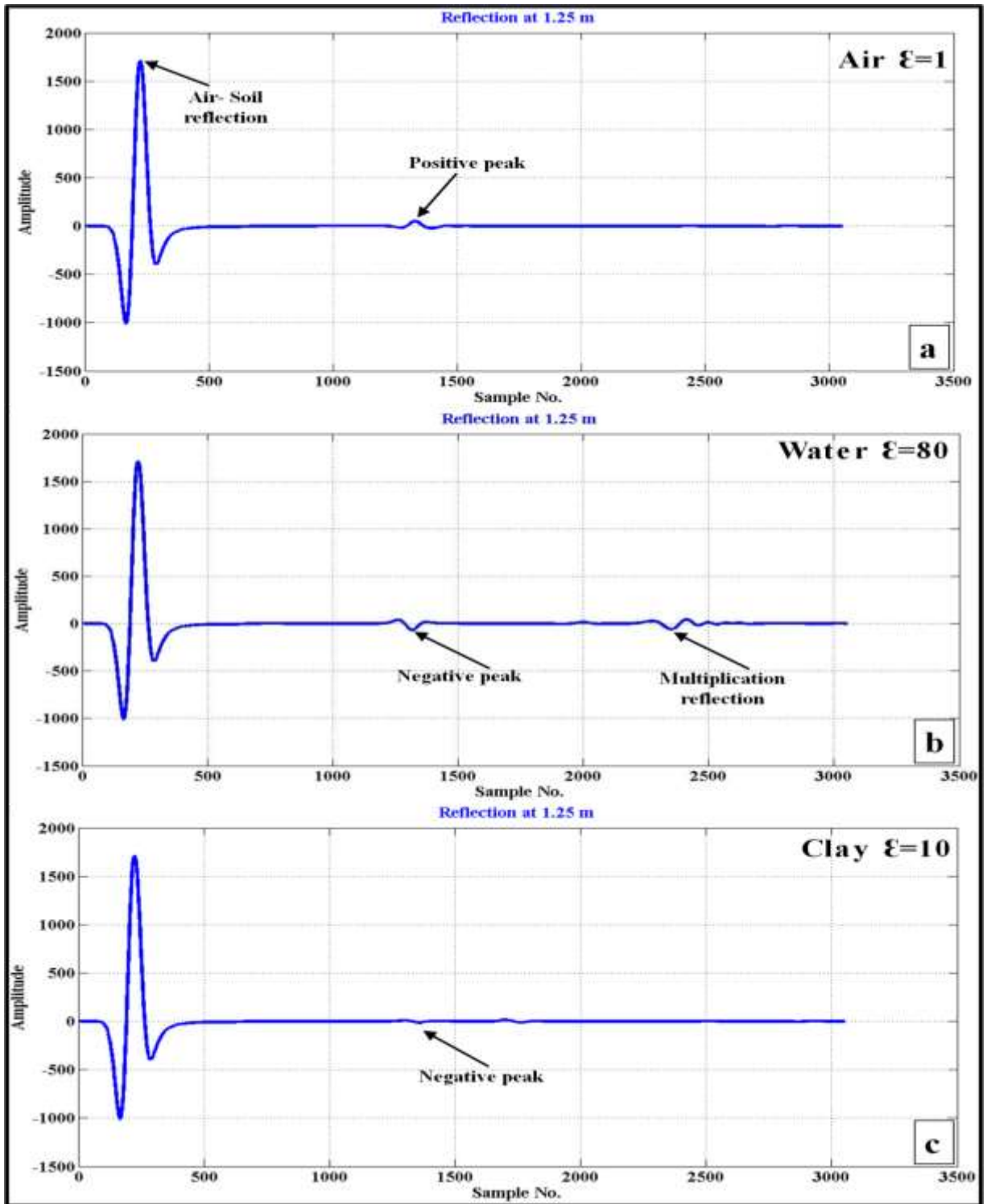


Figure (13):a, one scan across air-filled pipe, b, one scan across water-filled pipe, and c, one scan across clay-filled pipe.

The fourth model represents three subsurface pipes with different sizes and located under different depths. The synthetic result shows just the water-filled and air-filled pipes reflections but the reflection of the clay-filled pipe is undetectable due to the high depth of this pipe. Also, the hyperbola size has a direct proportion with the pipe size and its depth (Annan, 2001).

The fifth model synthetic result shows the reflections from the water-filled and air-filled pipes reflections that have a same size and different depths. The clay-filled pipe is not found due to the high depth of it. The lower side of the water-filled pipe reflection is clear due to the small size of this pipe.

The sixth model represents three subsurface pipes with different sizes and buried under the same depth. The synthetic result shows the reflection from the top of all three pipes and the hyperbola sizes for the clay-filled pipe is larger than the water-filled and the second one is larger than the air-filled pipe which is due to the pipe size.

## **Conclusions**

Six simulated models for several subsurface pipes have been simulated by using the GPRMaxV2.0 and the chosen antenna was the 900MHz antenna due to its high resolution. These models represent three pipe situations, healthy pipe which filled with water, empty pipe (air-filled pipe) and unhealthy and leaked pipe (clay-filled pipe). From the simulation synthetic data, all the pipes were detectable except the deepest pipe (the fourth and fifth model) due to the 900MHz antenna penetration depth. This problem can be solved by using a higher frequency antenna such as 400MHz antenna. The reflection strength is due to the



reflection coefficient between the host media and the filled material, in the simulated models the water-filled pipe has the highest reflection with a large negative peak and the clay-filled pipe has a weak reflection strength with a large negative peak, while the air-filled pipe has a weak reflection strength with a large positive peak. The hyperbola shape was depending on the pipe size, pipe depth, and the surrounding materials, the more size and the more depth has the larger and wider hyperbola.

### **References**

Annan A.P., (2001). Ground Penetrating Radar Workshop Notes. Sensors & Software Inc.

Carcione, J. M., (1996). Ground-radar numerical modeling applied to engineering problems. *European Journal of Environmental and Engineering Geophysics*. 1: 65-85.

Carcione, J. M., (1998). Radiation patterns for 2-D forward modeling. *Geophysics*. 63(2): 424-430.

Carcione, J. M., Schoenberg, M. A., (2000). 3-D Ground-penetrating radar simulation and plane-wave theory in anisotropic media. *Geophysics*. 65(5): 1527-154.

Giannopoulos, A., (2005). Modeling ground penetrating radar by GPRMax. *Construction and Building Materials*. 19(10): 755-762.

Lampe, B., Holliger, K., Green, A. G., (2003). A finite-difference time-domain simulation tool for ground-penetrating radar antennas. *Geophysics*. 68(3): 971-987.

Luebbers, R. J., Hunsberger, F., (1992). FDTD for nth-order dispersive media. *IEEE Transaction on Antenna Propagation*. 40(11): 1297–1301.

Olhoeft, G. R., (2003). Electromagnetic Field and Material Properties in Ground Penetrating Radar. Proceedings of the 2nd international workshop on advanced GPR, Delft, Netherlands, 144-147.

Reynolds. John M., (1998). An Introduction to Applied and Environmental Geophysics. Wiley, New York.

Roberts, R. L., Daniels, J. J. (1996). Analysis of GPR polarization phenomena. Journal of Environmental and Engineering Geophysics. 1(2): 139-157.

Su, M. M., (2013). Identification and Estimation of Concentration of Metal Bearing Minerals in Lunar Soil Using Ground Penetrating Radar, PhD. Thesis, College of Science and Mathematics, University of Arkansas at Little Rock, Arkansas, USA.

Teixeira, F. L., Chew, W. C., Straka, M., Oristaglio, M. L., (1998). Finite-difference time-domain simulation of ground-penetrating radar on dispersive, inhomogeneous, and conductive soils. IEEE Transactions on Geoscience and Remote Sensing. 36:1928–1937.

Xu, T., McMechan, G. A., (1997). GPR attenuation and its numerical simulation in 2.5 dimensions. Geophysics. 62(1): 403-414.

Yee, K. S., (1966). Numerical solution of initial boundary value problems involving Maxwell's Equations in isotropic media. IEEE Transactions on Antennas and Propagation. 14(3): 302-307.

## قابلية الرادار المخترق للاعماق في التعرف على حالة الانابيب تحت السطحية: محاكاة بالحاسب الالي

### الخلاصة

في الوقت الحاضر، فشل المجاري والانابيب تحت السطحية تعتبر واحدة من اهم المشاكل الشائعة في العراق، ومن الصعوبة تحديد مواقع هذه الانابيب تحت السطح لغرض اصلاحها او تبديلها. من المعروف ان الطرق الجيوفيزيائية تلعب دورا مهما لاستكشاف الشواذ والاهداف المدفونه تحت السطح وتحديد مواقعها. جهاز الرادار المخترق للاعماق يعتبر احد الاجهزة والوسائل المهمة لتحديد واستكشاف الاهداف تحت السطحية.

قبل الخروج للحقل واجراء المسوحات والاستكشاف يبدأ عمل المحاكاة بالحاسب الالي. العديد من الموديلات النظرية صممت في هذه الدراسة من اجل دراسة امكانية جهاز الرادار المخترق للاعماق في اكتشاف الانابيب تحت السطحية ومعرفة حالتها و مقاساتها (الحجم، العمق، المواد المألثة لها). تم استخدام برنامج الجي بي ار ماكس الاصدار الثاني في هذه المحاكاة. النماذج النظرية المصممه عباره عن انابيب تحت سطحية مختلفة الاحجام والاعماق والمواد المألثة. المواد المألثة كانت الهواء والاطيان والماء. اعتماداً على هذه المحاكاة يمكننا ان نستنتج بان جهاز الرادار المخترق للاعماق له القدره على استكشاف الانابيب تحت سطحية وايضا له القدرة على تحديد احجام الانابيب واشكالها واعماقها. ايضا ان جهاز الرادار المخترق للاعماق له القدرة على التمييز بين المواد المألثة لهذه الانابيب.